Millisecond Catalytic Reforming of Monoaromatics over Nobel Metals

C. M. Balonek, J. L. Colby, and L. D. Schmidt
Dept. of Chemical Engineering and Materials Science, University of Minnesota, 421 Washington Ave. SE, Minneapolis, MN 55455

DOI 10.1002/aic.12045
Published online August 24, 2009 in Wiley InterScience (www.interscience.wiley.com).

The millisecond autothermal reforming of benzene, toluene, ethylbenzene, cumene, and styrene were independently studied over five noble metal-based catalysts: Pt, Rh, Rh/γ-Al_2O_3, Rh–Ce, and Rh–Ce/γ-Al_2O_3, as a function of carbon-to-oxygen feed ratio. The Rh–Ce/γ-Al_2O_3 catalyst exhibited the highest feedstock conversion as well as selectivities to both synthesis gas and hydrocarbon products (lowest selectivities to H_2O and CO_2). Experimental results demonstrate a high stability of aromatic rings within the reactor system. Benzene and toluene seem to react primarily heterogeneously, producing only syngas and combustion products. Ethylbenzene and cumene behaved similarly, with higher conversions than benzene and toluene, and high product selectivity to styrene, likely due to homogeneous reactions involving their alkyl groups. Styrene exhibited low conversions over Rh–Ce/γ-Al_2O_3, emphasizing the stability of styrene in the reactor system. © 2009 American Institute of Chemical Engineers *AIChE J,* 56: 979–988, 2010

Keywords: reactor, catalysis, autothermal, monoaromatic, benzene, toluene, ethylbenzene, cumene, styrene, rhodium

Introduction

Aromatic compounds are frequently found in the polymer structures of biomass, particularly in the lignin component, and commodity plastics. An understanding of their catalytic degradation would provide insight for their utilization and processing. Gasification of biomass to synthesis gas (syngas) is a promising route for producing renewable fuels and chemicals; however, undesired tar byproducts require energy intensive cleanup stages.[1] At $\geq$60 wt% of total contaminants, aromatics such as benzene and toluene are commonly used as research models for tars.[1,2] Additionally, pyrolysis and gasification of plastic wastes have recently been examined as an alternative production route to fuels and chemicals. Specifically, pyrolysis of polystyrene has been shown to produce large amounts of styrene monomer and other aromatics.[3–6]

Correspondence concerning this article should be addressed to L. D. Schmidt at schmi001@cems.umn.edu

Understanding the decomposition of monoaromatics is also important as they are released from many industrial and combustion processes. Aromatic compounds are highly toxic and environmentally harmful, causing acid rain and increasing low atmosphere ozone levels.[7,8] The release of aromatic compounds can be largely attributed to the use of transportation fuels, which can contain up to 35% aromatics, added to increase octane rating, which reduces engine knock.

Research involving the high temperature pyrolysis or oxidation of monoaromatic species is limited. Brooks et al., Alzueta et al., and Da Costa et al. studied the gas-phase pyrolysis and oxidation of benzene.[7–9] Brooks et al. also studied gas-phase ethylbenzene pyrolysis and observed hydrogen and styrene as the primary products.[10] Pant et al. observed toluene pyrolysis with steam to produce methane, benzene, bibenzyl, and carbon oxides with coke yields $\leq$10.4%.[11]

Noble metal-based catalysts have previously been shown to convert a variety of fuels autothermally on millisecond time scales with up to 100% conversion and no coke formation.[12–15] This work examines the effect of catalyst, support, and carbon-to-oxygen feed ratio during the autothermal

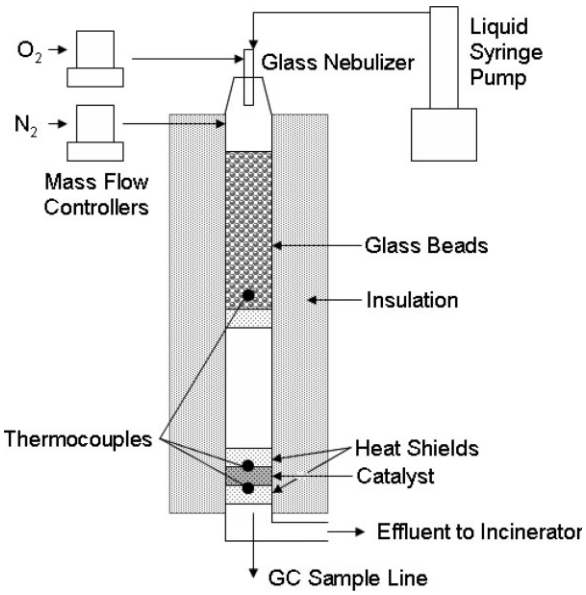

Figure 1. Schematic of apparatus used for monoaromatic experiments.

catalytic conversion of monoaromatics (benzene, toluene, ethylbenzene, cumene, and styrene) over noble metal-based catalysts (Rh and Pt) to investigate the behavior of aromatic rings and the role of substituted groups within the reactor system.

Experimental

Monoaromatics were autothermally reformed in a 19 mm ID quartz tube reactor system (Figure 1). Nitrogen and oxygen at air stoichiometry were fed by Brooks 5850i mass flow controllers and monitored using LabView 6.1. Liquid monoaromatics were fed by an ISCO 500D syringe pump ($\pm$0.001 mL min^{-1}) and completely vaporized using a glass neblulizer (Precision Glassblowing) and a 20 cm heated bed of glass beads (200 $\pm$ 5 °C) 27 cm upstream of the catalyst. Liquid flows were typically 1 to 3 mL min^{-1}.

Two uncoated α-Al_2O_3 45 pores per linear inch (ppi) monoliths were placed at the front and back face of the catalyst as heat shields and friction fit in the reactor tube using 1 mm thick ceramic insulation. Temperatures at the catalyst front and back face, and throughout the system, were measured using type-K thermocouples and monitored with LabView. The entire apparatus was wrapped in 2.5 cm thick ceramic fiber insulation to minimize heat loss (typically $\leq$15%). Reactor effluent was immediately and completely incinerated.

Catalyst preparation

All catalysts were deposited on 1.6 cm diameter, 1 cm long cylindrical 45 ppi α-Al_2O_3 monoliths. Rh (2.5 wt%) was applied to a blank monolith as aqueous Rh $(NO_3)_3$ using the incipient wetness technique, dried, then calcined for 6 h at 600 °C.[16] Rh–Ce catalysts (2.5 wt% each) were prepared by the same method, with Ce deposited as $Ce(NO_3)_3 \cdot 6H_2O$. For washcoated catalysts, 5 wt% washcoat was applied by aqueous slurry of γ-Al_2O_3 powder then calcined before application of desired metal. Pt (2.5 wt%) was loaded as aqueous H_2PtCl_6, dried, then reduced under H_2 and N_2 at 500 °C for 6 h. All Rh-based catalysts were run for $\geq$60 h without noticeable deactivation.

Reactor startup and operation

The apparatus was first externally heated under nitrogen flow sufficiently above the boiling point of the liquid feed. The desired flow conditions were chosen based on the feed C/O ratio, defined as the ratio of the inlet carbon atoms to the inlet oxygen atoms. C/O ratios between 1.0 (fuel lean) and 3.0 (fuel rich), in increments of 0.2, were tested for each feed and catalyst combination. The total inlet flow was held constant at 4 SLPM with N_2 and O_2 at air stoichiometry. C/O = 1.6 was chosen for reactor startup to be outside the combustion zone and to prevent coke formation.

Once the reactor was heated and the desired feed ratio was flowing, an isolated portion of the catalyst was heated externally to $\sim$250 °C with a butane torch to begin autothermal catalytic reaction of the feed. The heat and reaction then propagated throughout the catalyst bed, noted by a dramatic increase in catalyst temperature. After reactor startup, the system was allowed to reach steady state for 30 min before data acquisition.

Reactor shutdown was initiated by turning off the oxygen, followed by the liquid feed. Nitrogen was flowed at 2 SLPM until the entire system cooled below 150 °C.

Data acquisition and analysis

Products were sampled directly below the catalyst bed through a quartz capillary to a stainless steel line heated to 200 $\pm$ 5 °C, preventing effluent condensation. The residence time in the sample line was varied to confirm there was negligible downstream chemistry during sampling.

An HP 6890 Gas Chromatograph equipped with autosampling, a 30 m, 320 μm ID HP-Plot Q capillary column, and a thermal conductivity detector was used to identify and quantify permanent gases, C_2 hydrocarbons, and unreacted monoaromatics.

Three effluent samples (generally $\leq$5% carbon error each) were analyzed and averaged for each data point. Product selectivities were measured and defined as the ratio of atoms in the product species to the atoms in the converted aromatic feed. Unidentified effluent species were grouped according to number of carbon atoms (verified by a separate HP 5890 Gas Chromatograph Mass Spectrometer with the same column) and used to estimate carbon error. To ensure data reproducibility and negligible catalyst deactivation, C/O ratios were repeated periodically and duplicate catalysts were tested.

Results

Each of the five monoaromatic feeds were tested on each of the five noble metal-based catalysts. Benzene, toluene, ethylbenzene, and cumene were run stably on all Rh-based catalysts with no observable coke formation. Experiments on Pt catalysts were unsuccessful due to coking and will not be

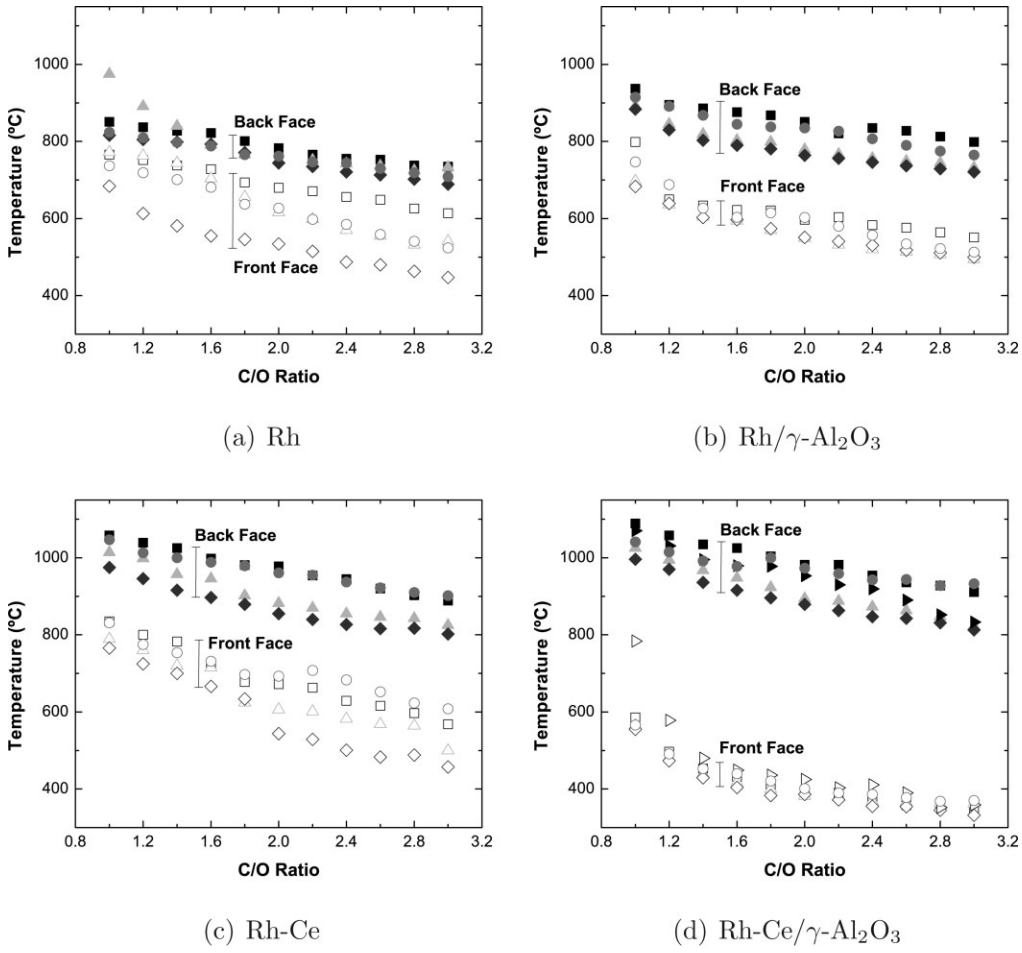

Figure 2. Front (open) and back (filled) face catalyst temperatures for ■ benzene, ● toluene, ▲ ethylbenzene, ♦ cumene, and ▶ styrene on (a) Rh, (b) Rh/γ-Al_2O_3, (c) Rh–Ce, and (d) Rh–Ce/γ-Al_2O_3.

included in references to "all data/experiments" hereafter. Styrene was run without severe coke formation on Rh–Ce/γ-Al_2O_3 only.

Catalyst temperatures

Catalyst back face temperatures were consistently hotter than the front face and both temperatures decreased as C/O ratio increased for all experiments (Figure 2). All feeds produced similar catalyst temperatures, although benzene and toluene typically had higher temperatures than ethylbenzene and cumene (~50–100 °C). The Rh catalyst had the smallest axial temperature gradient, as well as the lowest back face temperatures. Generally, catalyst back face temperatures increased and front face temperatures decreased in the order of Rh/γ-Al_2O_3, Rh–Ce, and Rh–Ce/γ-Al_2O_3.

Conversion

Conversion of each feed decreased as C/O ratio increased (Figure 3). Benzene and toluene behaved very similarly on all catalysts with the lowest conversions of all fuels. Ethylbenzene and cumene had consistently higher conversion, reaching 100% at low C/O ratios on some catalysts. Styrene conversions on Rh–Ce/γ-Al_2O_3 were similar to benzene and toluene. Conversion increased in the order of Rh < Rh/γ-Al_2O_3 < Rh–Ce < Rh–Ce/γ-Al_2O_3.

Hydrogen selectivity

Benzene and toluene produced similar selectivity to hydrogen-containing products, as did ethylbenzene and cumene. For all experiments, hydrogen selectivity to H_2 (S_{H_2}) decreased with increasing C/O ratio (Figures 4 and 5). As benzene and toluene generally produced only hydrogen and water, changes in S_{H_2} were met with equal and opposite changes in selectivity to water. Ethylbenzene and cumene had lower S_{H_2}, as a variety of hydrocarbons were observed in the effluent. Styrene converted on Rh–Ce/γ-Al_2O_3 had a large range of values for S_{H_2}, varying between ~20 and 80% over all C/O ratios.

The S_{H_2} was lowest on the Rh catalyst, generally $\leq$20% for all feeds, and highest on the Rh–Ce/γ-Al_2O_3 catalyst. Rh–Ce and Rh/γ-Al_2O_3 produced selectivities between these extremes, with Rh–Ce more selective to H_2 than Rh/γ-Al_2O_3 for benzene and toluene.

Carbon selectivity

Carbon oxides. Very similar carbon selectivities were observed for benzene and toluene as well as ethylbenzene

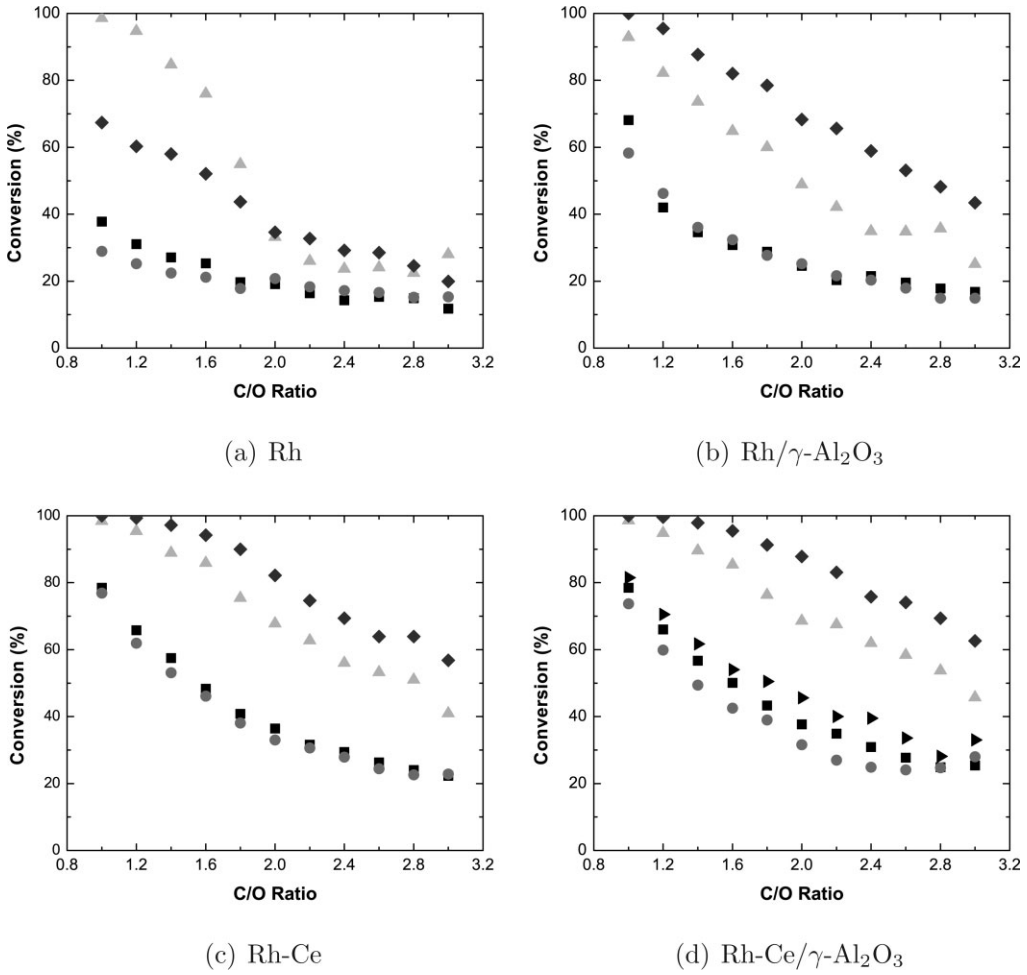

Figure 3. Percent fuel conversion of ■ benzene, ● toluene, ▲ ethylbenzene, ♦ cumene, and ▶ styrene on (a) Rh, (b) Rh/γ-Al_2O_3, (c) Rh–Ce, and (d) Rh–Ce/γ-Al_2O_3.

and cumene. For all experiments, S_{CO} was always higher than S_{CO_2}. Benzene exhibited the highest S_{CO} (Figure 6) and generally only produced carbon oxides. Toluene behaved similarly to benzene, although with a slightly smaller difference between S_{CO} on each catalyst. S_{CO} were similar for cumene and ethylbenzene. Styrene on Rh–Ce/γ-Al_2O_3 exhibited much higher S_{CO} than ethylbenzene or cumene.

Rh–Ce/γ-Al_2O_3 gave the highest S_{CO} for all feeds. Rh–Ce had the next highest S_{CO}, although performed similar to Rh–Ce/γ-Al_2O_3 below C/O of 1.6 for benzene and toluene. Rh had the lowest S_{CO}, whereas Rh/γ-Al_2O_3 performed between Rh and Rh–Ce.

Hydrocarbons. Benzene on Rh/γ-Al_2O_3 produced trace amounts ($\ll$1%) of methane, ethylene, and acetylene between C/O of 1.2 and 1.8. Only syngas and combustion products were observed for all other benzene experiments. Methane (<1%) and benzene (1–2%) were also observed in the toluene effluent for all experimental conditions.

Styrene was consistently the most abundant hydrocarbon product for both ethylbenzene and cumene (Figure 7). For cumene, benzene, methane, and ethylene were the next three most abundant hydrocarbon products with selectivities $\leq$11, 5, and 6%, respectively. All other species exhibited selectivities less than 2.5%. For ethylbenzene, benzene, toluene, and ethylene were the next three most abundant hydrocarbon products with selectivities $\leq$14, 11, and 7%, respectively. All other species were observed at trace amounts except for methane, which never exceeded a selectivity of 2.7%.

Styrene exhibited a low selectivity to hydrocarbons on Rh–Ce/γ-Al_2O_3. Carbon selectivity was highest to benzene and ethylene, $\leq$10 and 5%, respectively. Methane, acetylene, toluene, and ethylbenzene were also observed, but never exceeded a selectivity of 2.2%.

Discussion

Monoaromatics

Benzene and toluene. Benzene seems to react primarily at the catalyst surface with little homogeneous gas-phase reaction. Benzene adsorbs by π-bonding parallel to the Rh surface, typically over a three-fold hollow site with very limited molecular desorption.[17–21] Decomposition begins by C–C bond cleavage and surface carbon species can react with adsorbed oxygen.[18,20,21] The presence of hydrocarbon surface species facilitates carbon movement on the metal

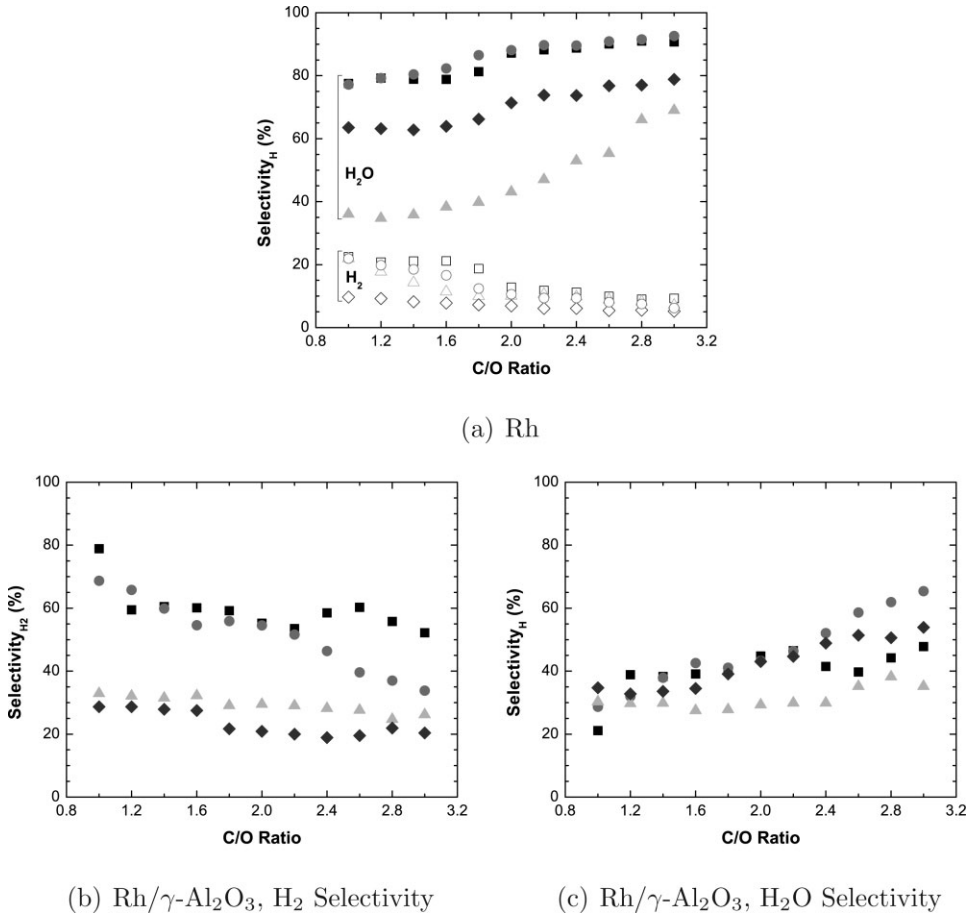

Figure 4. Hydrogen selectivity to H_2 and H_2O of ■ benzene, ● toluene, ▲ ethylbenzene, and ♦ cumene on (a) Rh, and (b), (c) Rh/γ-Al_2O_3.

surface for further reaction, limiting coke formation.[20] CO, CO_2, H_2, and H_2O are produced primarily through heterogeneous catalytic reactions.

The large bond dissociation energies and high resonance stability associated with an aromatic ring limit homogeneous reactions.[7] This stability requires higher temperatures and longer residence times to homogeneously react benzene than those present in the experimental system.[7,10] However, temperatures throughout the catalyst were sufficient to initiate benzene oxidation for all C/O ranges. Therefore, only trace amounts of benzene reacted homogeneously to produce methane, ethylene, and acetylene.[8,10]

Toluene has been shown previously to behave similar to benzene on metal catalytic surfaces, in agreement with the presented experimental results.[19–22] For all catalysts and feed ratios, benzene and toluene had nearly identical conversions and selectivities. Carbon selectivity to methane and benzene from toluene were 1 – 2% for all C/O ratios, likely produced from homogeneous reactions, as routes to products $>C_1$ on Rh from toluene are unknown at the presented experimental conditions.[18,19]

Ethylbenzene and cumene. Addition of a functional group to an aromatic ring can increase homogeneous and heterogeneous reactivity.[23,24] The larger alkyl groups and the weak secondary and tertiary C–H bonds of ethylbenzene and cumene can participate in homogeneous reactions and also adsorb more favorably onto the catalyst surface than benzene. Homogeneous reactions of these alkyl groups produce the wide range of hydrocarbons observed in the effluent during experiments.[25]

Ethylbenzene and cumene had similar conversion trends on all catalysts (Figure 3), excluding low C/O ratios on Rh. Both fuels consistently had higher conversion than benzene or toluene due to higher homogeneous reactivity. High styrene selectivity (Figure 7) may indicate homogeneous dehydrogenation of ethylbenzene for all experiments. Benzene and ethylene may have been produced by homogeneous cleavage of the alkyl group from the aromatic ring. Toluene and methane were also observed as gas phase products. Of the converted fuel, at least one-third survived as an aromatic ring.

Cumene generally had higher conversion than ethylbenzene due to the increased homogeneous reactivity of the larger alkyl group. Again, styrene was the major homogeneous product, resulting from the cleavage of one carbon from the isopropyl group. Benzene and ethylene were also observed in equal molar amounts in the effluent of cumene experiments, possibly as a result of further homogeneous reaction of styrene.

Styrene. On Rh–Ce/γ-Al_2O_3, styrene exhibited conversion similar to that of toluene and benzene across all C/O

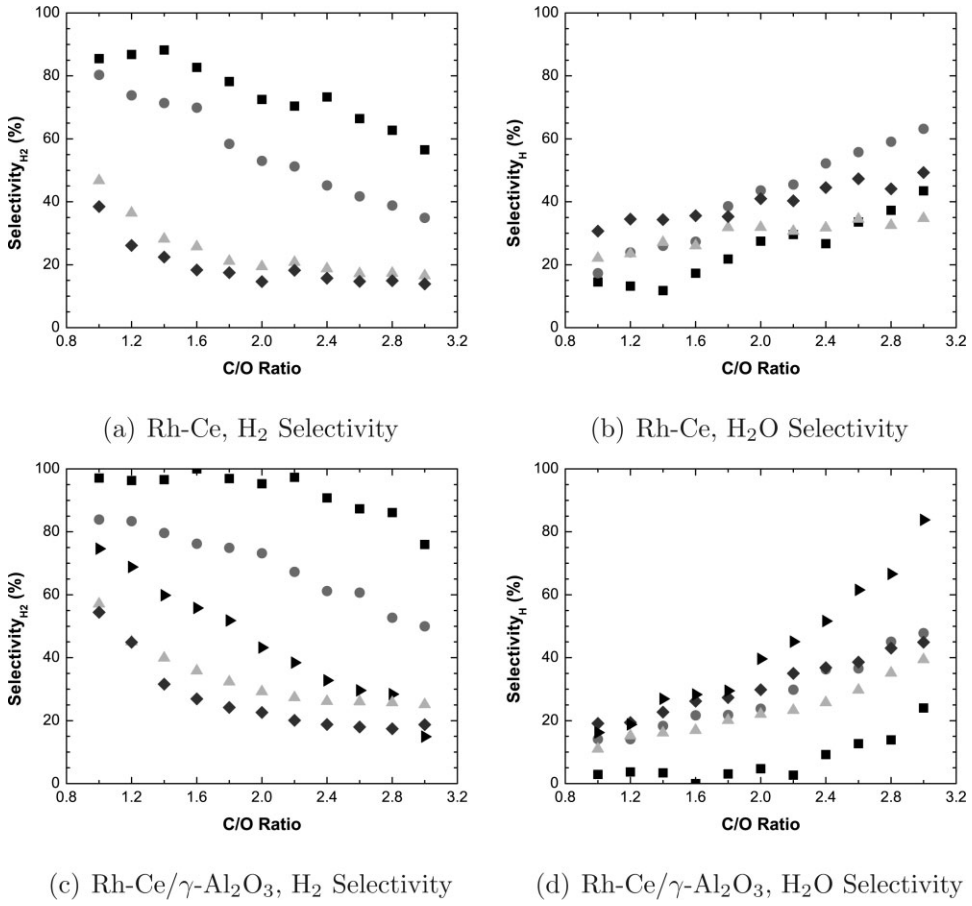

Figure 5. Hydrogen selectivity to H_2 and H_2O of ■ benzene, ● toluene, ▲ ethylbenzene, ♦ cumene, and ▶ styrene on (a), (b) Rh–Ce, and (c), (d) Rh–Ce/γ-Al_2O_3.

ratios, much lower than ethylbenzene or cumene (Figure 3). Hydrogen and carbon oxide species were the main products, resulting primarily from catalytic reactions. The only hydrocarbon selectivities larger than ~2% were those to benzene and ethylene, resulting from the homogeneous cleaving of the ethenyl group from the aromatic ring. The high selectivity to styrene of both ethylbenzene and cumene in combination with styrene's lower conversion may indicate a higher gas phase stability, resulting from the higher bond energy associated with the carbon double bond of the ethenyl group.

Catalysts

Platinum. Data were not collected on Pt catalysts due to severe coking and catalyst deactivation during operation. Benzene and other aromatics adsorb on Pt in the same manner as on Rh.[17,26] However, C–H bonds are the first to break on Pt, rather than the C–C bonds.[20,26,27] The formation of strong C–C networks and the lack of mobile C–H surface species contribute to the formation of unreactive coke, which deactivates the catalyst.

Pt was successfully lit off, but deactivated within 90 s of startup. Deactivation likely began at the front face (as indicated by an initial front face temperature drop) where cooler temperatures facilitated solid carbon formation. Catalyst coking propagated rapidly through the catalyst, quenching the reaction. Similar results were observed previously.[28]

Rhodium. The rhodium catalyst reformed all monoaromatics autothermally, excluding styrene, to a mixture of syngas and hydrocarbons.

Generally, benzene and toluene were observed to have higher front and back face temperatures than the higher alkylated aromatics (excluding styrene on Rh–Ce/γ-Al_2O_3). Reforming reactions with steam generated in the catalyst bed and endothermic homogeneous cracking of ethylbenzene, cumene, and their gas phase products may have resulted in lower temperatures throughout the catalyst (Figure 2). The higher gas phase stability of benzene, toluene, and styrene limited endothermic reactions, maintaining high catalyst temperatures.

Rh generally exhibited high S_{CO}, especially for benzene and toluene (Figure 6). Ethylbenzene and cumene exhibited lower S_{CO} due to their high gas-phase reactivity to hydrocarbons. S_{CO_2} was very similar for all feeds and much lower than S_{CO}. As discussed earlier, the majority of carbon oxide products are believed to be produced on the catalyst surface. High temperatures observed at low C/O ratios reduce species' surface residence time on the catalyst, resulting in higher fuel conversion and higher selectivity to CO, as CO will more likely desorb on Rh than react with an additional surface oxygen.[20] As C/O ratio increases, the system

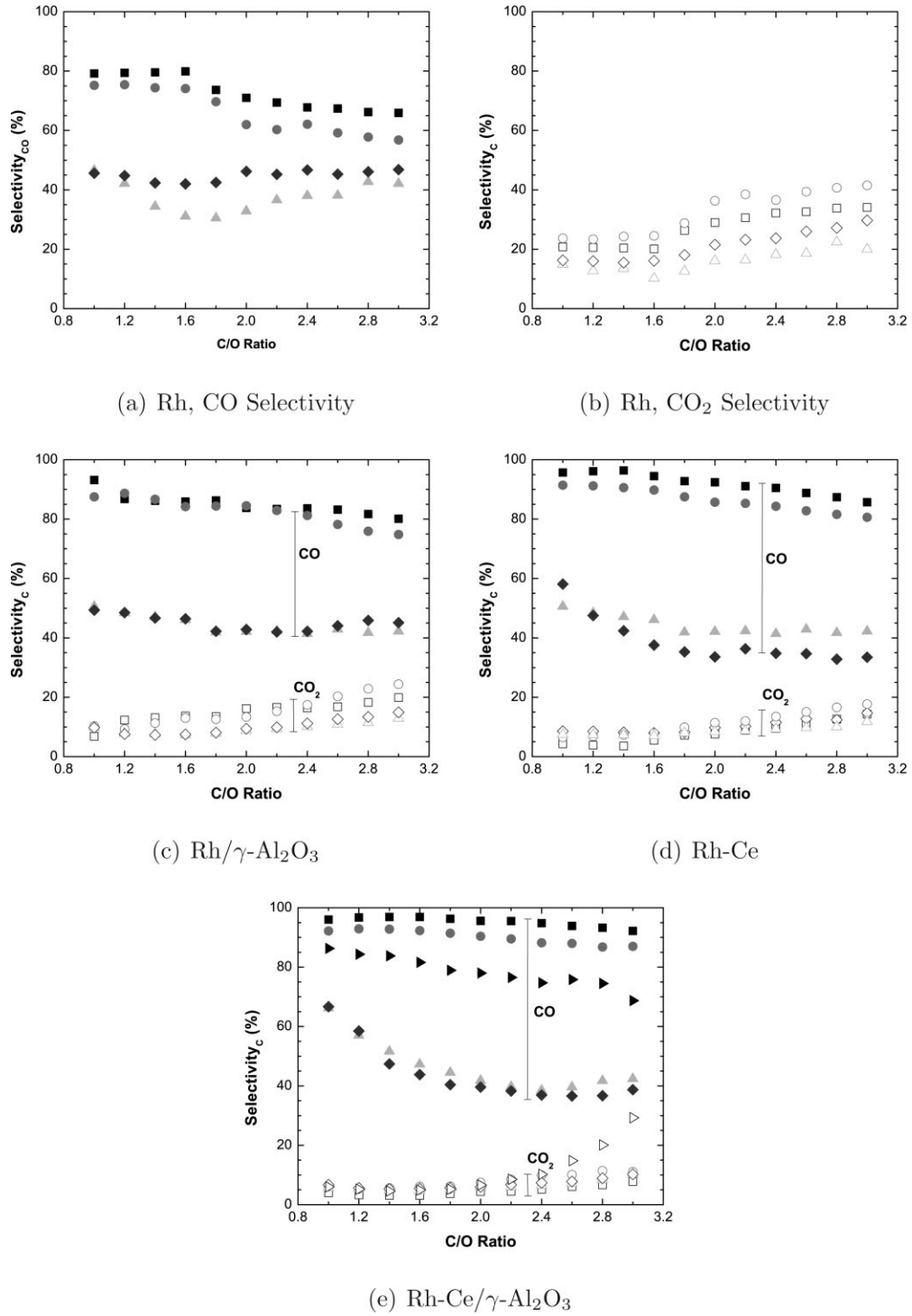

Figure 6. Carbon selectivity to CO (filled) and CO_2 (open) of ■ benzene, ● toluene, ▲ ethylbenzene, ♦ cumene, and ▶ styrene on (a), (b) Rh, (c) Rh/γ-Al_2O_3, (d) Rh–Ce, and (e) Rh–Ce/γ-Al_2O_3.

becomes more fuel rich, decreasing temperatures and lengthening the surface residence time, producing more CO_2 and less CO.

Similar to S_{CO}, S_{H_2} on Rh was highest for benzene and toluene (Figure 4). However, S_{H_2O} was consistently higher than S_{H_2} for all feeds, possibly due to reactions of O_2 with desorbed H_2 throughout the catalyst bed. Ethylbenzene and cumene had lower S_{H_2} and S_{H_2O} than benzene and toluene due to their high selectivity to hydrocarbons.

Rh/γ-Al_2O_3. The addition of a γ-Al_2O_3 washcoat to Rh catalysts has been shown to increase catalytic sites and maintain catalytic performance at high temperatures by preventing metal sintering.[13,16,29] Compared with the Rh catalyst, the addition of a washcoat increased benzene and

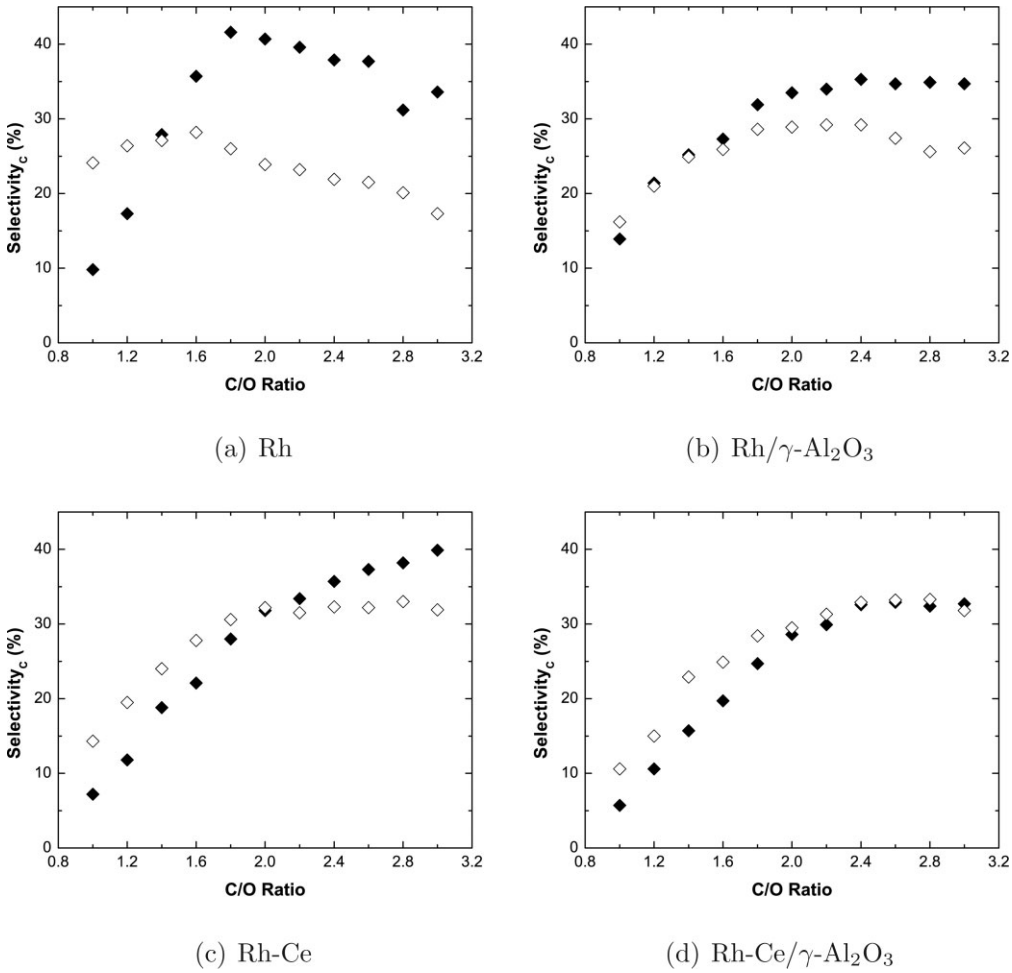

Figure 7. Carbon selectivity to styrene of ethylbenzene (filled) and cumene (open) on (a) Rh, (b) Rh/γ-Al_2O_3, (c) Rh–Ce, and (d) Rh–Ce/γ-Al_2O_3.

toluene back face temperatures by ~60–80 °C and conversions by ~10% at all C/O ratios (Figures 2 and 3). Despite an increase in conversion for ethylbenzene and cumene as well, the back face temperature of Rh/γ-Al_2O_3 was very similar to Rh. This may be due to higher rates of endothermic homogeneous cracking balancing the increase in exothermic catalytic conversion.

Washcoat addition generally decreased the catalyst front face temperature. This change, although only ~20 °C, may be caused by an increase in reforming at the front face. Rh has been shown to be a very active steam reforming catalyst, and the addition of washcoat increases reforming activity by increasing the number of catalyst sites.[30] The increase in catalytic activity also increased the selectivity to syngas products for all feeds. A dramatic increase in S_{H_2} was observed, especially for benzene and toluene, which was matched by an equal drop in S_{H_2O} (Figure 4).

Rh–Ce. Cerium addition to a Rh catalyst has been shown to stabilize the Rh metal, increase catalyst selectivities to syngas, and prevent coke formation by increasing oxidation rates at the surface.[13,29,31–34] For all fuels, addition of Ce gave the same, or slightly higher front face temperatures than the Rh catalyst. However, the back face temperatures increased dramatically, higher than either Rh or Rh/γ-Al_2O_3 by 100 – 200 °C (Figure 2). Overall conversions for all fuels were also significantly higher at all C/O ratios.

For benzene and toluene, Ce addition increased selectivity to syngas and decreased S_{H_2O} and S_{CO_2} more than the addition of a washcoat (Figures 4–6). However, the selectivity differences between Ce and washcoat addition were difficult to distinguish for ethylbenzene and cumene due to the high rates of homogeneous chemistry for both.

Rh–Ce/γ-Al_2O_3. The Rh–Ce/γ-Al_2O_3 catalyst was the only catalyst able to reform styrene for all C/O ratios without severe coke formation. This catalyst also experienced the largest temperature gradient of all catalysts. The front face temperature was significantly lower, below 400 °C at high C/O ratios (Figure 2). As with Rh/γ-Al_2O_3, the lower temperatures may be explained by an increase in endothermic steam reforming activity at the front face, facilitated by washcoat addition.[12] The back face temperatures and conversions, higher than both Rh and Rh/γ-Al_2O_3, were very similar to those of the Rh–Ce catalyst. Addition of Ce to Rh seems to have a stronger effect on increasing exothermic surface oxidation reaction rates than does addition of washcoat.

For benzene and toluene, Rh–Ce/γ-Al_2O_3 had the highest selectivity to syngas and the lowest to H_2O and CO_2 of any

catalyst (Figures 4–6). The same was true for ethylbenzene and cumene; however, the difference was considerably smaller. The combination of washcoat and Ce increased catalytic sites and activity to maximize syngas selectivity and minimize total oxidation products.

Conclusions

Benzene and toluene behave similarly on all catalysts and they generally react heterogeneously to produce syngas and combustion products. Toluene produces small amounts of benzene and methane, primarily from homogeneous reactions. Ethylbenzene and cumene also behave similarly, with high conversion and large amounts of hydrocarbon and aromatic products (mostly styrene) due to homogeneous reactivity of the alkyl group. Styrene conversion was similar to benzene and toluene possibly due to higher homogeneous stability than ethylbenzene and cumene. Styrene was only stably reformed on Rh–Ce/γ-Al_2O_3, mainly producing syngas and combustion products with small amounts of benzene and ethylene. Overall, the aromatic ring was very stable in the reactor.

Comparing catalyst performance, Pt coked severely and deactivated for each feed tested. Rh successfully converted monoaromatics, excluding styrene, autothermally on millisecond time scales. Back face temperatures were consistently higher than the front face due to heat produced from oxidation reactions throughout the catalyst. The addition of a γ-Al_2O_3 washcoat stabilized Rh catalyst sites, lowering the front face temperature because of an increase in endothermic steam reforming activity, and producing higher overall conversions and syngas selectivities. The addition of Ce more effectively increased conversion and syngas selectivity than washcoat for benzene and toluene. However, selectivity differences between Rh–Ce and Rh/γ-Al_2O_3 for ethylbenzene and cumene were unclear due to their high selectivities to homogeneous products. Fuel conversion and back face temperatures were very similar between Rh–Ce and Rh–Ce/γ-Al_2O_3. However, Rh–Ce/γ-Al_2O_3 produced the highest selectivities to syngas of any catalyst and was the only catalyst able to convert styrene.

Finally, product selectivities can be adjusted by changing the C/O ratio. Low C/O ratios (fuel lean) produced higher temperatures, conversions, and syngas selectivities. Higher C/O ratios resulted in lower conversions and temperatures and higher selectivities to hydrocarbon and combustion products.

Acknowledgments

This article is based on work supported under a National Science Foundation Graduate Research Fellowship. This work was also partially supported by U.S. Department of Energy Grant DE-FG02-88ER13878.

Literature Cited

1. Osipovs S. Sampling of benzene in tar matrices from biomass gasification using two different solid-phase sorbents. *Anal Bioanal Chem.* 2008;391:1409–1417.
2. Carpenter DL, Deutch SP, French RJ. Quantitative measurement of biomass gasifier tars using a molecular-beam mass spectrometer; Comparison with traditional impinger sampling. *Energy Fuels.* 2007; 21:3036–3043.
3. Ward PG, Goff M, Donner M, Kaminsky W, O'Connor KE. A two step chemo-biotechnological conversion of polystyrene to a biodegradable thermoplastic. *Environ Sci Technol.* 2006;40:2433–2437.
4. Liu Y, Qian J, Wang J. Pyrolysis of polystyrene waste in a fluidized-bed reactor to obtain styrene monomer and gasoline fraction. *Fuel Process Technol.* 2000:63:45–55.
5. Kaminsky W, Predel M, Sadiki A. Feedstock recycling of polymers by pyrolysis in a fluidised bed. *Polym Degrad Stab.* 2004;85:1045–1050.
6. Williams PT, Williams EA. Recycling plastic waste by pyrolysis. *J Inst Energy.* 1998;71:81–93.
7. Alzueta MU, Glarborg P, Dam-Johansen K. Experimental and kinetic modeling study of the oxidation of benzene. *Int J Chem Kinet.* 2000;32:498–522.
8. Da Costa I, Fournet R, Billaud F, Battin-Leclerc F. Experimental and modeling study of the oxidation of benzene. *Int J Chem Kinet.* 2003;35:503–524.
9. Brooks CT, Peacock SJ, Reuben BG. Pyrolysis of benzene. *J Chem Soc J Farad Trans 1 Phys Chem Condens Phases.* 1979;75:652–62.
10. Brooks CT, Peacock SJ. Pyrolysis of ethylbenzene. *J Chem Soc Farad Trans 1 Phys Chem Condens Phases.* 1982;78:3187–3202.
11. Pant KK, Kunzru D. Noncatalytic and catalytic pyrolysis of toluene. *Can J Chem Eng.* 1999;77:150–155.
12. Donazzi A, Michael BC, Schmidt LD. Chemical and geometric effects of Ce and washcoat addition on catalytic partial oxidation of CH_4 on Rh probed by spatially resolved measurements. *J Catal.* 2008;260:270–275.
13. Degenstein NJ, Subramanian R, Schmidt LD. Partial oxidation of n-hexadecane at short contact times: catalyst and washcoat loading and catalyst morphology. *Appl Catal A Gen.* 2006;305:146–159.
14. Dauenhauer PJ, Dreyer BJ, Degenstein NJ, Schmidt LD. Millisecond reforming of solid biomass for sustainable fuels. *Angew Chem.* 2007;46:5864–5867.
15. Colby JL, Dauenhauer PJ, Schmidt LD. Millisecond autothermal steam reforming of cellulose for synthetic biofuels by reactive flash volatilization. *Green Chem.* 2008;10:773–783.
16. Bodke AS, Bharadwaj SS, Schmidt LD. The effect of ceramic supports on partial oxidation of hydrocarbons over noble metal coated monoliths. *J Catal.* 1998;179:138–149.
17. Koel BE. A high-resolution electron energy loss spectroscopy study of the surface structure of benzene adsorbed on the rhodium(lll) crystal face. *J Phys Chem.* 1984;88:1988–1996.
18. Koel BE. Thermal decomposition of benzene on the Rh(111) crystal surface. *J Phys Chem.* 1986;90:2949–2956.
19. Minot C, Gallezot P. Competitive hydrogenation of benzene and toluene: theoretical study of their adsorption on ruthenium, rhodium, and palladium. *J Catal.* 1990;123:341–348.
20. Viste ME, Gibson KD, Sibener SJ. Heterogeneous combustion of benzene on Rh(lll): kinetics and dynamics of CO and CO2 production. *J Catal.* 2000;191:237–244.
21. Ioannides T, Verykios XE. The interaction of benzene and toluene with Rh dispersed on SiO_2, Al_2O_3, and TiO_2 carriers. *Catal.* 1993;143:175–186.
22. Friend CM, Muetterties EL. Coordination chemistry of metal surfaces. 3. Benzene and toluene interactions with nickel surfaces. *J Am Chem Soc.* 1981;103:773–779.
23. Patterson MJ, Angove DE, Cant NW. The effect of carbon monoxide on the oxidation of four C6 to C8 hydrocarbons over platinum, palladium and rhodium. *Appl Catal B Environ.* 2000;26:47–57.
24. Patterson MJ, Angove DE, Cant NW. The effect of metal order on the oxidation of a hydrocarbon mixture over alumina-supported combined platinum/rhodium catalysts. *Appl Catal B Environ.* 2001; 35:53–58.
25. Domke SB, Pogue RF, Van Neer FJR, Smith CM. Investigation of the kinetics of ethylbenzene pyrolysis using a temperature-scanning reactor. *Ind Eng Chem Res.* 2001;40:5878–5884.
26. Tsai M-C, Muetterities EL. Coordination chemistry of benzene, toluene, cyclohexadienes, cyclohexene, and cyclohexane on Pt(100). *J Phys Chem.* 1982;86:5067–5071.
27. Duprez D, Miloudi A, Delahay G, Maurel R. Selective steam reforming of aromatic hydrocarbons. *J Catal.* 1986;101:56–66.
28. Torniainen PM, Chu X, Schmidt LD. Comparison of monolith-supported metals for the direct oxidation of methane to syngas. *J Catal.* 1994;146:1–10.

29. Dauenhauer PJ, Salge JR, Schmidt LD. Renewable hydrogen by autothermal steam reforming of volatile carbohydrates. *J Catal*. 2006;244:238–247.
30. Duprez D. Selective steam reforming of aromatic compounds on metal catalysts. *Appl Catal A Gen*. 1992;82:111–157.
31. Wheeler C, Jhalani A, Klein EJ, Tummala S, Schmidt LD. The water-gas-shift reaction at short contact times. *J Catal*. 2004;223:191–199.
32. Salge JR, Deluga GA, Schmidt LD. Catalytic partial oxidation of ethanol over noble metal catalysts. *J Catal*. 2005;235:69–78.
33. Cordatos H, Bunluesin T, Stubenrauch J, Vohs JM, Gorte RJ. Effect of ceria structure on oxygen migration for Rh/ceria catalysts. *J Phys Chem*. 1996;100:785–789.
34. Zhu T, Flytzani-Stephanopoulos M. Catalytic partial oxidation of methane to synthesis gas over Ni-CeO_2. *Appl Catal A Gen*. 2001; 208:403–417.

Manuscript received May 27, 2009, and revision received July 16, 2009.